Available online at www.sciencedirect.com
ScienceDirect
Trans. Nonferrous Met. Soc. China 25(2015) 293−302
Transactions of Nonferrous Metals Society of China
www.tnmsc.cn

Three-dimensional analytical solution of acoustic emission source location for cuboid monitoring network without pre-measured wave velocity

Long-jun DONG[1,2], Xi-bing LI[1], Zi-long ZHOU[1], Guang-hui CHEN[1], Ju MA[1]

1. School of Resources and Safety Engineering, Central South University, Changsha 410083, China;
2. Australian Centre for Geomechanics, The University of Western Australia, Perth 6009, Australia

Received 27 August 2013; accepted 25 November 2014

Abstract: To find analytical solutions of nonlinear systems for locating the acoustic emission/microseismic(AE/MS) source without knowing the wave velocity of structures, the sensor location coordinates were simplified as a cuboid monitoring network. Different locations of sensors on upper and lower surfaces were considered and used to establish nonlinear equations. Based on the proposed functions of time difference of arrivals, the analytical solutions were obtained using five sensors under three networks. The proposed analytical solutions were validated using authentic data of numerical tests and experiments. The results show that located results are consistent with authentic data, and the outstanding characteristics of the new solution are that the solved process is not influenced by the wave velocity knowledge and iterated algorithms.

Key words: acoustic emission; seismic source; sensor; location; analytical solution

1 Introduction

It is generally accepted that most solids emit low-level seismic signals when they are stressed or deformed. The solution of the problem of locating a signal source using time difference of arrival (TDOA) measurements has numerous applications in aerospace, surveillance, structural health, navigation, industrial process, speaker location, machine condition, monitoring of nuclear explosions, and mining induced areal seismology [1,2]. In the geotechnical field, this phenomenon is generally referred to as acoustic emission/microseismic (AE/MS) activities. When rock fractures, it produces AE/MS signals that transmit through the rock as elastic waves [3−5]. The application of the AE/MS system, which monitors self-generated acoustic signals occurring within the ground, has now rapidly increased for the monitoring of underground structures such as mines [6−8], tunnels [9−12], natural gas, nuclear engineering, and petroleum storage caverns, as well as surface structures such as foundations, rock, and soil slopes [13−16].

The location of a seismic event (earthquake, MS or AE) has been the first and most basic step in any study of seismicity on any scale since 1910 [17]. In general, earthquakes are predicted for their source locations, defined by the coordinates and the origin time, assuming a seismic velocity model and minimizing the difference between the observed and the calculated travel times. Source location is one of the classic problems in seismic areas [18,19]. Considerable number of studies published in the past more than 100 years on seismic source location have proved the importance and, at the same time, the complexity of this problem.

Many researchers have developed different AE/MS/seismic source location techniques, and some of which have been mature technologies and widely used in the positioning of AE/MS currently[20−23], for example the joint hypocenter determination method, the double-difference method, and topographic inverse [24−26]. Nevertheless, the problem of determining the four source parameters (geocentric: x, y, z and origin time) has still not be definitively solved. The iterative analytic procedures, which are nowadays most often used for the calculation (cf. Geiger's method), are not infrequently divergent, or at any rate do not give very reliable results, which considerably reduces the number of well-located

Foundation item: Projects (11447242, 41272304, 51209236, 51274254) supported by the National Natural Science Foundation of China; Project (2015CB060200) supported by the National Basic Research Program of China
Corresponding author: Long-jun DONG ; Tel: +86-13973160861; E-mail: rydong001@csu.edu.cn
DOI: 10.1016/S1003-6326(15)63604-4

events. This can lead to negative consequences when interpreting the activity itself. It is well-known that the correct location of the source is dramatically hindered by the following factors: 1) insufficient knowledge of the seismic wave velocity; 2) inadequate distribution of the stations; 3) intrinsic limitations of the iteration algorithm applied. Generally, those factors do not act independently each other. Taking Geiger's algorithm which is actually the widely used and known one as an example, the use of initial evaluated hypocenter coordinates is presupposed, and an iterative least-square technique is used. These conditions significantly influence the location accuracy.

DONG and LI [27] proposed a set of analytical solutions for the AE/MS source location under a cuboid monitoring network of sensor location. A location method with P-wave velocity by analytical solutions (P-VAS) was obtained with the established equations. Virtual location tests show that the relocation results of analytical method are fully consistent with the actual coordinates for events both inside and outside the monitoring network; whereas the location error of traditional time difference method is between 0.01 and 0.03 m for events inside the sensor array, and the location errors are large, which are up to 1080986 m for events outside the sensor arrays. The broken pencil location tests were carried out in a granite rock specimen with 350 mm in length and the cross section of 100 mm×98 mm, using five AE sensors. Five AE sources were relocated with the conventional method and the P-VAS method. For the four events outside monitoring network, the positioning accuracy by the P-VAS method is higher than that by the traditional method, and the location accuracy of the larger one can be increased by 17.61 mm. The results of both virtual and broken pencil location tests show that their resolved analytical solutions are effective to improve the positioning accuracy. However, the problem of the P-VAS is that the wave velocity should be given in advance. It is difficult to apply in the conditions without pre-measured velocity or pre-given velocity knowledge.

In this work, the analytical solutions of the AE/MS source location coordinates without the knowledge of wave velocity were developed. Different locations of sensors on upper and lower surfaces were considered and used to establish nonlinear equations. Based on the proposed functions of time difference of arrivals, the analytical solutions were obtained using five sensors under several networks without need of wave velocity. The method highlights three outstanding advantages: 1) without using iterative solution; 2) without initial evaluated hypocenter coordinates; 3) without pre-measured velocity or pre-given velocity knowledge.

2 Statement of problem and solution method

The AE/MS/seismic source location method using P-wave arrival time is widely used to calculate source coordinates for two reasons: the fastest propagation velocity, and the easy identification of first arrival time. The AE/MS/seismic source location coordinate is (x, y, z); T_i(i=1, 2, ⋯, n) is the ith monitoring station, and its coordinate is (x_i, y_i, z_i) (i=1, 2, ⋯, n); l_i(i=1, 2, ⋯, n) is the distance from the AE/MS/seismic source to the station T_i; t_i(i=1, 2, ⋯, n) is the arrival time recorded by sensor in the station T_i; t_0 is the origin time of AE/MS source. Then, t_i can be expressed as

$$t_i = \frac{l_i}{v} + t_0 \tag{1}$$

where v is the P-wave velocity.

By the spatial distance formula between two points (the source location and the monitoring station location), it can be obtained

$$l_i = \sqrt{(x_i - x)^2 + (y_i - y)^2 + (z_i - z)^2} \tag{2}$$

By taking Eq. (2) into Eq. (1), we have

$$(t_i - t_0)v = \sqrt{(x_i - x)^2 + (y_i - y)^2 + (z_i - z)^2} \tag{3}$$

In Eq. (3), t_i(i=1, 2, ⋯, n), v, and (x_i, y_i, z_i) (i=1, 2, ⋯, n) are known; the seismic or AE source (x, y, z) and origin time t_0 are unknown, which are needed to be solved. By taking each station data to Eq. (3), an equation can be obtained. Four stations correspond to four equations, and they can constitute a set of nonlinear equations. Generally, the greater the number of station is, the higher the positioning accuracy is. In the past more than 100 years, most researches were focused on the nonlinear optimization or iteration methods to locate the AE/MS/seismic source. The location precision was greatly influenced by the error of the wave velocity and the intrinsic limitations of the iteration algorithm applied. In this work, in order to find out the analytical solution of the AE/MS/seismic source location coordinates, the sensor location coordinates were optimized and simplified.

A cuboid monitoring network of sensor locations was selected, and the AE/MS/seismic source localization equations were established. The sensors are required to install at the vertices of the cuboid monitoring network. There are two cases including four sensors installed on one surface and additional one sensor on another surface (Fig. 1) as well as three sensors installed on one surface and additional two sensors on another surface (Fig. 2).

For every surface of the first case (Fig. 1), there are four types of monitoring network including Figs. 1(a),

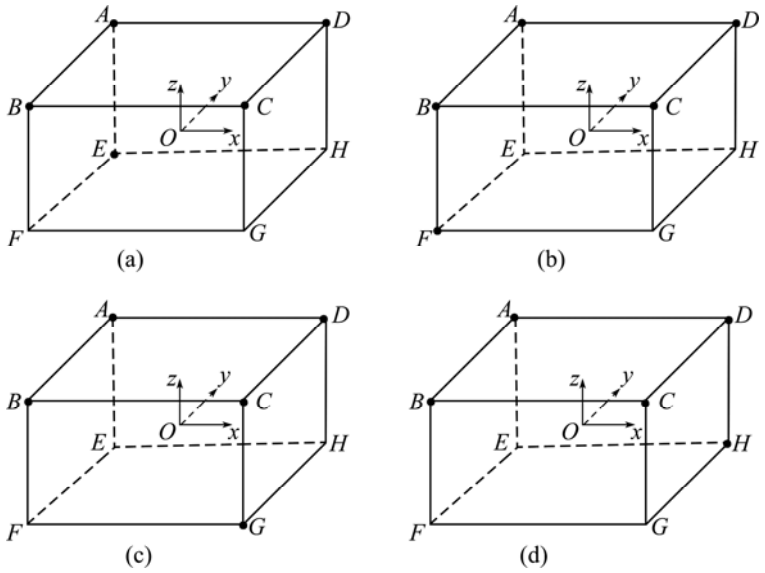

Fig. 1 Three-dimensional location schematic of cuboid monitoring network: (a) AE sensors at vertices *A*, *B*, *C*, *D* and *E*; (b) AE sensors at vertices *A*, *B*, *C*, *D* and *F*; (c) AE sensors at vertices *A*, *B*, *C*, *D* and *G*; (d) AE sensors at vertices *A*, *B*, *C*, *D* and *H*

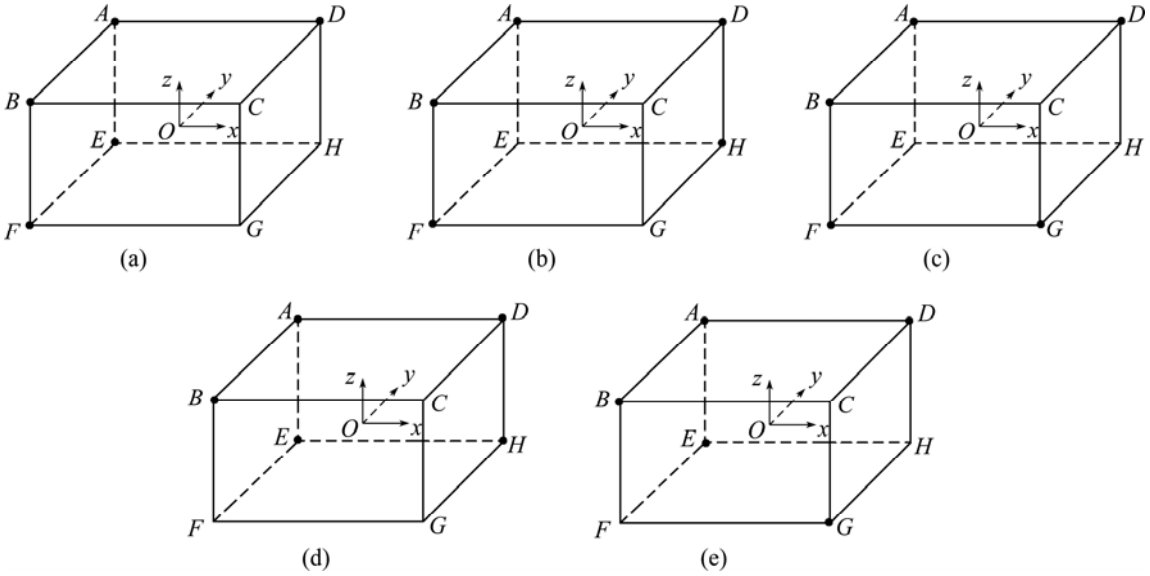

Fig. 2 Three-dimensional location schematic of cuboid monitoring network: (a) AE sensors at vertices *A*, *B*, *D*, *E* and *F*; (b) AE sensors at vertices *A*, *B*, *D*, *F* and *H*; (c) AE sensors at vertices *A*, *B*, *D*, *F* and *G*; (d) AE sensors at *A*, *B*, *D*, *E*, *H*; (e) AE sensors at vertices *A*, *B*, *D*, *E* and *G*

(b), (c) and (d). The first type (Fig. 1(a)) is analyzed in this work, and the others are similar. Five sensors are installed at vertices *A*, *B*, *C*, *D* and *E* of the cuboid monitoring network. The center of the cuboid is taken as the coordinate origin, and the coordinate direction is shown in Fig. 1.

The lengths of three sides of the monitoring network cuboid are 2*a*, 2*b* and 2*c*, respectively. The first sensor *A* is taken as a reference. The travel time of the sensor *A* from an AE/MS/seismic event is expressed as t_{10}, and the arrival time of sensors *B*, *C*, *D* and *E* is $t_{10}+\Delta t_2$, $t_{10}+\Delta t_3$, $t_{10}+\Delta t_4$, and $t_{10}+\Delta t_5$, respectively. According to Eq. (3), it can be obtained

$$(a+x)^2+(b-y)^2+(c-z)^2=v^2{t_{10}}^2 \tag{4}$$

$$(a+x)^2+(b+y)^2+(c-z)^2=v^2(t_{10}+\Delta t_2)^2 \tag{5}$$

$$(a-x)^2+(b+y)^2+(c-z)^2=v^2(t_{10}+\Delta t_3)^2 \tag{6}$$

$$(a-x)^2+(b-y)^2+(c-z)^2=v^2(t_{10}+\Delta t_4)^2 \tag{7}$$

$$(a+x)^2+(b-y)^2+(c+z)^2=v^2(t_{10}+\Delta t_5)^2 \tag{8}$$

Taking subtraction of Eqs.(4) and (5), Eqs. (4) and (6), Eqs. (4) and (7), as well as Eqs. (4) and (8), we have

$$4by = v^2(2t_{10}\Delta t_2 + \Delta t_2{}^2) \tag{9}$$

$$-4ax+4by = v^2(2t_{10}\Delta t_3 + \Delta t_3{}^2) \tag{10}$$

$$-4ax = v^2(2t_{10}\Delta t_4 + \Delta t_4{}^2) \tag{11}$$

$$-4cz = -v^2(2t_{10}\Delta t_4 + \Delta t_4{}^2) \tag{12}$$

From Eqs. (9) , (10) , and (11) one can easily obtain

$$(2t_{10}\Delta t_2 + \Delta t_2{}^2) + (2t_{10}\Delta t_4 + \Delta t_4{}^2) = (2t_{10}\Delta t_3 + \Delta t_3{}^2) \tag{13}$$

Resolving Eq. (13) yields

$$t_{10} = \frac{\Delta t_3^2 - \Delta t_2^2 - \Delta t_4^2}{2(\Delta t_2 + \Delta t_4 - \Delta t_3)} \tag{14}$$

Taking the ratio of Eq. (9) to Eq. (11), we have

$$y = \frac{-a(2t_{10}\Delta t_2 + \Delta t_2{}^2)}{b(2t_{10}\Delta t_4 + \Delta t_4{}^2)}x \tag{15a}$$

Supposing $l = \dfrac{2t_{10}\Delta t_2 + \Delta t_2{}^2}{2t_{10}\Delta t_4 + \Delta t_4{}^2}$, Eq. (15a) can be rewritten as

$$y = \frac{-al}{b}x \tag{15b}$$

From Eqs. (11) and (12) one can obtain

$$z = \frac{-a(2t_{10}\Delta t_5 + \Delta t_5{}^2)}{c(2t_{10}\Delta t_4 + \Delta t_4{}^2)}x \tag{16}$$

Supposing $m = \dfrac{2t_{10}\Delta t_5 + \Delta t_5{}^2}{2t_{10}\Delta t_4 + \Delta t_4{}^2}$, Eq. (16) can be rewritten as

$$z = -\frac{am}{c}x \tag{17}$$

Eq. (4) divided by Eq. (9), we have

$$\frac{(a+x)^2 + (b-y)^2 + (c-z)^2}{4by} = \frac{t_{10}{}^2}{(2t_{10}\Delta t_2 + \Delta t_2{}^2)} \tag{18}$$

Supposing $n = \dfrac{t_{10}^2}{2t_{10}\Delta t_2 + \Delta t_2{}^2}$, and substituting Eqs. (15a) and (17) into Eq. (18), we have

$$\left[\left(\frac{a}{b}l\right)^2 + \left(\frac{a}{c}m\right)^2 + 1\right]x^2 + \left(2a + 2al + 2am+4aln\right)x + a^2 + b^2 + c^2 = 0 \tag{19}$$

Eq. (19) can be rewritten as

$$Ax^2 + Bx + C = 0 \tag{20}$$

where

$$A = \left[\left(\frac{a}{b}l\right)^2 + \left(\frac{a}{c}m\right)^2 + 1\right], B = \left(2a + 2al + 2am+4aln\right),$$

and $C=a^2+b^2+c^2+$.

Then, x, y, and z can be obtained by resolving Eqs. (20), (15b) and (17). The solutions can be defined as analytical solution I (ASI).

For every surface of the second case in Fig. 2, there are five types of monitoring network including Figs. 2(a), (b), (c), (d) and (e). The first type (Fig. 2(a)) is analyzed in this work, and the others are similar. Five sensors are installed at vertices A, B, D, E, and F of the cuboid monitoring network. The center of the cuboid is taken as the coordinate origin, and the coordinate direction is shown in Fig. 2. The lengths of three sides of the monitoring network cuboid are $2a_s$, $2b_s$ and $2c_s$, respectively. The first sensor A is taken as a reference. The travel time from an AE/MS/seismic source (x_s, y_s, z_s) to sensor A is expressed as t_{s10}, and the arrival time of sensors B, D, E and F is $t_{s10}+\Delta t_{s2}$, $t_{s10}+\Delta t_{s3}$, $t_{s10}+\Delta t_{s4}$ and $t_{s10}+\Delta t_{s5}$, respectively. The P-wave velocity is expressed as v_s. According to Eq. (3), it can be obtained

$$(a_s+x_s)^2 + (b_s - y_s)^2 + (c_s - z_s)^2 = v_s{}^2 t_{s10}{}^2 \tag{21}$$

$$(a_s+x_s)^2 + (b_s+y_s)^2 + (c_s - z_s)^2 = v_s{}^2(t_{s10} + \Delta t_{s2})^2 \tag{22}$$

$$(a_s - x_s)^2 + (b_s - y_s)^2 + (c_s - z_s)^2 = v_s{}^2(t_{s10} + \Delta t_{s3})^2 \tag{23}$$

$$(a_s+x_s)^2 + (b_s - y_s)^2 + (c_s+z_s)^2 = v_s{}^2(t_{s10} + \Delta t_{s4})^2 \tag{24}$$

$$(a_s + x_s)^2 + (b_s + y_s)^2 + (c_s + z_s)^2 = v_s{}^2(t_{s10} + \Delta t_{s5})^2 \tag{25}$$

Taking subtraction of Eqs. (21) and (22), Eqs. (21) and (23), Eqs. (21) and (24), as well as Eqs. (21) and (25), we have

$$4b_s y_s = v_s{}^2\ (2t_{s10}\Delta t_{s2} + \Delta t_{s2}{}^2\ ) \tag{26}$$

$$4a_s x_s = -v_s{}^2\ (2t_{s10}\Delta t_{s3} + \Delta t_{s3}{}^2\ ) \tag{27}$$

$$4c_s z_s = v_s{}^2\ (2t_{s10}\Delta t_{s4} + \Delta t_{s4}{}^2\ ) \tag{28}$$

$$4b_s y_s + 4c_s z_s = v_s{}^2\ (2t_{s10}\Delta t_{s5} + \Delta t_{s5}{}^2\ ) \tag{29}$$

From Eqs. (26), (28), and (29) one can easily obtain

$$(2t_{s10}\Delta t_{s2} + \Delta t_{s2}{}^2) + (2t_{s10}\Delta t_{s4} + \Delta t_{s4}{}^2) = 2t_{s10}\Delta t_{s5} + \Delta t_{s5}{}^2 \tag{30}$$

$$t_{s10} = \frac{\Delta t_{s5}{}^2 - \Delta t_{s2}{}^2 - \Delta t_{s4}{}^2}{2(\Delta t_{s2} + \Delta t_{s4} - \Delta t_{s5})} \tag{31}$$

From Eqs. (26) and (27) one can obtain

$$y_s = -\frac{a_s}{b_s}\left(\frac{2t_{s10}\Delta t_{s2} + \Delta t_{s2}{}^2}{2t_{s10}\Delta t_{s3} + \Delta t_{s3}{}^2}\right)x_s \tag{32}$$

Supposing $l_s=\dfrac{2t_{s10}\Delta t_{s2}+\Delta t_{s2}{}^2}{2t_{s10}\Delta t_{s3}+\Delta t_{s3}{}^2}$, Eq. (32) can be rewritten as

$$y_s=-\frac{a_s l_s}{b_s}x_s \tag{33}$$

From Eqs. (28) and (27) one can obtain

$$z_s=-\frac{a_s}{c_s}\left(\frac{2t_{s10}\Delta t_{s4}+\Delta t_{s4}{}^2}{2t_{s10}\Delta t_{s3}+\Delta t_{s3}{}^2}\right)x_s \tag{34}$$

Supposing $m_s=\dfrac{2t_{s10}\Delta t_{s4}+\Delta t_{s4}{}^2}{2t_{s10}\Delta t_{s3}+\Delta t_{s3}{}^2}$, Eq. (34) can be rewritten as

$$z_s=\frac{-a_s m_s}{c_s}x_s \tag{35}$$

From Eqs. (21) and (26) one can obtain

$$\frac{(a_s+x_s)^2+(b_s-y_s)^2+(c_s-z_s)^2}{4b_s y_s}=\frac{t_{s10}{}^2}{(2t_{s10}\Delta t_{s2}+\Delta t_{s2}{}^2)} \tag{36}$$

Supposing $n_s=\dfrac{t_{s10}{}^2}{(2t_{s10}\Delta t_{s2}+\Delta t_{s2}{}^2)}$, and substituting Eqs. (33) and (35) in Eq. (36), we have

$$\left[\left(\frac{a_s}{b_s}l_s\right)^2+\left(\frac{b_s}{c_s}m_s\right)^2+1\right]x_s{}^2+(2a_s+2a_s l_s+2a_s m_s+4a_s n_s l_s)x_s+a_s{}^2+b_s{}^2+c_s{}^2=0 \tag{37}$$

Equation (37) can be rewritten as

$$A_s x_s{}^2+B_s x_s+C_s=0 \tag{38}$$

where

$$A_s=\left(\frac{a_s}{b_s}l_s\right)^2+\left(\frac{b_s}{c_s}m_s\right)^2+1,\ B_s=2a_s+2a_s l_s+2a_s m_s+4a_s n_s l_s,$$

and $C_s=a_s{}^2+b_s{}^2+c_s{}^2$. x_s, y_s, and z_s can be obtained by resolving Eqs. (38), (33) and (35), respectively. The solutions can be defined as analytical solution II (ASII).

It is noted that the above two conditions are different networks which considered both upper and lower surfaces of the cuboid with five sensors. The first case is four sensors on upper surface and one sensor on the lower surface, while the second case is three sensors on upper surface and two sensors on the lower surface. The first case has four types of networks and the second one has five types of networks. It is easy to find the different and significant characteristics between the two types of networks. If we consider six surfaces of the cuboid networks, we can see that the two selected conditions have the same characteristic, four and one sensors on two different surfaces. It is noted that the condition that two and three sensors on two different surfaces is not considered. To fix the problem systematically, the third condition, two sensors on one surface and three sensors on another surface (Fig. 2(b)), is analyzed and the analytical solution is also obtained.

The lengths of three sides of the monitoring network cuboid are $2a_p$, $2b_p$ and $2c_p$, respectively. The first sensor A is taken as a reference. The travel time from the AE/MS/seismic source (x_p, y_p, z_p) to the sensor A is expressed as $t_{p10,}$ and the arrival time of sensors A, B, D, F and H is $t_{p10}+\Delta t_{p2}$, $t_{p10}+\Delta t_{p3}$, $t_{p10}+\Delta t_{p4}$ and $t_{p10}+\Delta t_{p5}$, respectively. The P-wave velocity is expressed as v_p. According to Eq. (3), it can be obtained

$$(a_p+x_p)^2+(b_p-y_p)^2+(c_p-z_p)^2=v_p{}^2 t_{p10}{}^2 \tag{39}$$

$$(a_p+x_p)^2+(b_p+y_p)^2+(c_p-z_p)^2=v_p{}^2(t_{p10}+\Delta t_{p2})^2 \tag{40}$$

$$(a_p-x_p)^2+(b_p-y_p)^2+(c_p-z_p)^2=v_p{}^2(t_{p10}+\Delta t_{p3})^2 \tag{41}$$

$$(a_p+x_p)^2+(b_p+y_p)^2+(c_p+z_p)^2=v_p{}^2(t_{p10}+\Delta t_{p4})^2 \tag{42}$$

$$(a_p-x_p)^2+(b_p-y_p)^2+(c_p+z_p)^2=v_p{}^2(t_{p10}+\Delta t_{p5})^2 \tag{43}$$

Taking subtraction of Eqs. (39) and (40), Eqs. (39) and (41), Eqs. (39) and (42), as well as Eqs. (39) and (43), we have

$$4b_p y_p=v_p{}^2(2t_{p10}\Delta t_{p2}+\Delta t_{p2}{}^2) \tag{44}$$

$$4a_p x_p=-v_p{}^2(2t_{p10}\Delta t_{p3}+\Delta t_{p3}{}^2) \tag{45}$$

$$4b_p y_p+4c_p z_p=v_p{}^2(2t_{p10}\Delta t_{p4}+\Delta t_{p4}{}^2) \tag{46}$$

$$4a_p x_p-4c_p z_p=-v_p{}^2(2t_{p10}\Delta t_{p5}+\Delta t_{p5}{}^2) \tag{47}$$

From Eqs. (44), (45), and (46) one can easily obtain

$$(2t_{p10}\Delta t_{p2}+\Delta t_{p2}{}^2)-(2t_{p10}\Delta t_{p3}+\Delta t_{p3}{}^2)=(2t_{p10}\Delta t_{p4}+\Delta t_{p4}{}^2)-(2t_{p10}\Delta t_{p5}+\Delta t_{p5}{}^2) \tag{48}$$

$$t_{p10}=\frac{\Delta t_{p4}{}^2-\Delta t_{p5}{}^2-\Delta t_{p2}{}^2+\Delta t_{p3}{}^2}{2(-\Delta t_{p4}+\Delta t_{p5}+\Delta t_{p2}-\Delta t_{p3})} \tag{49}$$

Taking the ratio of Eq. (44) and Eq. (45), we have

$$y_p=-\frac{a_p}{b_p}\left(\frac{2t_{p10}\Delta t_{p2}+\Delta t_{p2}{}^2}{2t_{p10}\Delta t_{p3}+\Delta t_{p3}{}^2}\right)x_s \tag{50}$$

Supposing $l_s=\dfrac{2t_{p10}\Delta t_{p2}+\Delta t_{p2}{}^2}{2t_{p10}\Delta t_{p3}+\Delta t_{p3}{}^2}$, Eq. (50) can be rewritten as

$$y_{\mathrm{p}}=-\frac{a_{\mathrm{p}}l_{\mathrm{p}}}{b_{\mathrm{p}}}x_{\mathrm{p}} \tag{51}$$

Submitting Eq. (45) into Eq. (47) yields

$$-4c_{\mathrm{p}}z_{\mathrm{p}}=-{v_{\mathrm{p}}}^2(2t_{\mathrm{p10}}\Delta t_{\mathrm{p5}}+{\Delta t_{\mathrm{p5}}}^2)+{v_{\mathrm{p}}}^2(2t_{\mathrm{p10}}\Delta t_{\mathrm{p3}}+{\Delta t_{\mathrm{p3}}}^2) \tag{52}$$

Taking the ratio of Eq. (52) and Eq. (45), we have

$$z_{\mathrm{p}}=\frac{-a_{\mathrm{p}}\left[(2t_{\mathrm{p10}}\Delta t_{\mathrm{p5}}+{\Delta t_{\mathrm{p5}}}^2)-(2t_{\mathrm{p10}}\Delta t_{\mathrm{p3}}+{\Delta t_{\mathrm{p3}}}^2)\right]}{c_{\mathrm{p}}(2t_{\mathrm{p10}}\Delta t_{\mathrm{p3}}+{\Delta t_{\mathrm{p3}}}^2)}x_{\mathrm{s}} \tag{53}$$

Supposing

$$m_{\mathrm{p}}=\frac{(2t_{\mathrm{p10}}\Delta t_{\mathrm{p5}}+{\Delta t_{\mathrm{p5}}}^2)-(2t_{\mathrm{p10}}\Delta t_{\mathrm{p3}}+{\Delta t_{\mathrm{p3}}}^2)}{(2t_{\mathrm{p10}}\Delta t_{\mathrm{p3}}+{\Delta t_{\mathrm{p3}}}^2)},\ \text{Eq. (53)}$$

can be rewritten as

$$z_{\mathrm{p}}=\frac{-a_{\mathrm{p}}m_{\mathrm{p}}}{c_{\mathrm{p}}}x_{\mathrm{p}} \tag{54}$$

Taking the ratio of Eq. (39) and Eq. (44) yields

$$\frac{(a_{\mathrm{p}}+x_{\mathrm{p}})^2+(b_{\mathrm{p}}-y_{\mathrm{p}})^2+(c_{\mathrm{p}}-z_{\mathrm{p}})^2}{4b_{\mathrm{p}}y_{\mathrm{p}}}=\frac{{t_{\mathrm{p10}}}^2}{(2t_{\mathrm{p10}}\Delta t_{\mathrm{p2}}+{\Delta t_{\mathrm{p2}}}^2)} \tag{55}$$

Supposing $n_{\mathrm{p}}=\dfrac{{t_{\mathrm{p10}}}^2}{(2t_{\mathrm{p10}}\Delta t_{\mathrm{p2}}+{\Delta t_{\mathrm{p2}}}^2)}$, and substituting Eqs. (51) and (54) in Eq. (55), we have

$$\left[\left(\frac{a_{\mathrm{p}}}{b_{\mathrm{p}}}l_{\mathrm{p}}\right)^2+\left(\frac{b_{\mathrm{p}}}{c_{\mathrm{p}}}m_{\mathrm{p}}\right)^2+1\right]x_{\mathrm{p}}^2+(2a_{\mathrm{p}}+2a_{\mathrm{p}}l_{\mathrm{p}}+2a_{\mathrm{p}}m_{\mathrm{p}}+4a_{\mathrm{p}}n_{\mathrm{p}}l_{\mathrm{p}})x_{\mathrm{p}}+{a_{\mathrm{p}}}^2+{b_{\mathrm{p}}}^2+{c_{\mathrm{p}}}^2=0 \tag{56}$$

Eq. (56) can be rewritten as

$$A_{\mathrm{p}}{x_{\mathrm{p}}}^2+B_{\mathrm{p}}x_{\mathrm{p}}+C_{\mathrm{p}}=0 \tag{57}$$

where

$$A_{\mathrm{p}}=\left(\frac{a_{\mathrm{p}}}{b_{\mathrm{p}}}l_{\mathrm{p}}\right)^2+\left(\frac{a_{\mathrm{p}}}{c_{\mathrm{p}}}m_{\mathrm{p}}\right)^2+1,\ B_{\mathrm{p}}=2a_{\mathrm{p}}+2a_{\mathrm{p}}l_{\mathrm{p}}+2a_{\mathrm{p}}m_{\mathrm{p}}+4a_{\mathrm{p}}n_{\mathrm{p}}l_{\mathrm{p}},\ \text{and}\ C_{\mathrm{p}}={a_{\mathrm{p}}}^2+{b_{\mathrm{p}}}^2+{c_{\mathrm{p}}}^2.$$

x_{p}, y_{p} and z_{p} can be obtained by resolving Eqs. (57), (51) and (54), respectively. The solutions can be defined as analytical solution III (ASIII).

3 Validated examples and discussion

3.1 Numerical examples

In the first example, a positioning system includes five sensors at the five cuboid vertices, and the coordinates are *A*(−130, 165, 220), *B*(−130, −165, 220), *C*(130, −165, 220), *D*(130, 165, 220), *E*(−130, 165, −220). The average equivalent P-wave velocity in the medium is expressed as *v*, and *v*=5000 m/s. The AE/MS sources are *O*(110, 200, 180), *P*(210, 97, −89), *Q*(−77, −89, 190), *R*(−98, 22, 168), and *S*(99, −289, 190) (all coordinates have the length unit of m). The arrival time recorded by sensors is listed in Table 1, and the accuracy of time is 10^{-6} s. By using the proposed analytical solution to calculate the AE/MS source coordinates, coordinate values of the five sensors and arrival time of five sensors for five events are taken into Eqs. (20), (15b) and (17), and the coordinate values (*x*, *y*, *z*) of five acoustic emission events can be resolved. The actual and calculated results are listed in Table 2. It can be seen from Table 2, one set of the location results of the proposed analytical solutions are fully consistent with the actual coordinates.

In the second example, a positioning system includes five sensors at the five cuboid vertices, and the

Table 1 Arrival time recorded by sensors *O*, *P*, *Q*, *R*, and *S* in the first example

Sensor	Arrival time recorded by sensor /s				
	O	*P*	*Q*	*R*	*S*
A	0.049163	0.092888	0.052240	0.031098	0.101874
B	0.087733	0.105778	0.019478	0.039343	0.052428
C	0.073546	0.082589	0.044508	0.059886	0.026258
D	0.011358	0.065270	0.065807	0.054822	0.091209
E	0.093557	0.074131	0.097041	0.082950	0.130638

Table 2 Comparison between actual and calculated coordinates and errors of absolute distance in the first example

AE event	Actual coordinate/m			Calculated coordinate/m						Error of absolute distance/m	
				Solution 1			Solution 2				
	x	*y*	*z*	x_1	y_1	z_1	x_2	y_2	z_2	Solution 1	Solution 2
O	110	200	180	120.4569	219.0102	197.1033	109.9952	199.9892	179.9850	27.6271	0.0191
P	210	97	−89	316.3741	146.1332	−134.0807	209.9515	96.9766	−88.9783	125.5460	0.0581
Q	−77	−89	190	−77.0000	−89.0029	190.0056	−142.6235	164.8561	351.9387	0.0063	308.1777
R	−98	22	168	−97.9735	21.9956	167.9434	−236.7607	−53.1540	405.8485	0.0627	285.4375
S	99	−289	190	99.0027	−289.0048	190.0016	70.7758	206.6060	135.8298	0.0057	499.3559

coordinates are A(−130, 165, 220), B(−130, −165, 220), D(130, 165, 220), E (−130, 165, −220), and F(−130, −165, −220), and average equivalent P-wave velocity in the medium is expressed as v, and v=5000 m/s. Assume that AE/MS sources O, P, Q, R and S are as the same as the first example (all coordinates have the length unit of m). The arrival time recorded by sensors is listed in Table 3. By using the proposed analytical solution to calculate the AE/MS source coordinates, the coordinate values of the five sensors and arrival time of the five sensors for the five events are taken into Eqs. (38), (33) and (35), and the coordinate values (x_s, y_s, z_s) of five acoustic emission events can be resolved. The actual and calculated results are listed in Table 4. It can be seen from Table 4 that one set of the location results of the proposed analytical solutions are fully consistent with the authentic coordinates.

In the third example, a positioning system includes five sensors at the five cuboid vertices, and the coordinates are A(−130, 165, 220), B(−130, −165, 220), D(130, 165, 220), F (−130, −165, −220) and H(130, 165, −220). The average equivalent P-wave velocity in the medium is expressed as v, and v=5000 m/s. Assume that AE/MS sources O, P, Q, R and S are as the same as the first example (all coordinates have the length unit of m). The arrival time recorded by sensors is listed in Table 5. By using the proposed analytical solution to calculate the AE/MS source coordinates, the coordinate values (x_p, y_p, z_p) of the five sensor and arrival time of five sensors for the five events are taken into equations (57), (51) and (54), and the coordinate values of the five acoustic emission events can be resolved. The actual and calculated results are listed in Table 6. It can be seen

Table 3 Arrival time recorded by sensors A, B, D, E, and F in the second example

Sensor	Arrival time recorded by sensor/s				
	O	P	Q	R	S
A	0.049163	0.092888	0.052240	0.031098	0.101874
B	0.087733	0.105778	0.019478	0.039343	0.052428
D	0.011358	0.065270	0.065807	0.054822	0.091209
E	0.093557	0.074131	0.097041	0.082950	0.130638
F	0.118461	0.089756	0.084068	0.086380	0.097143

Table 4 Comparison between actual and calculated coordinates and errors of absolute distance in the second example

AE event	Actual coordinate/m			Calculated coordinate/m						Error of absolute distance/m	
				Solution 1			Solution 2				
	x	y	z	x_{s1}	y_{s1}	z_{s1}	x_{s2}	y_{s2}	z_{s2}	Solution 1	Solution 2
O	110	200	180	120.4483	218.9979	197.0923	110.0002	200.0013	179.9959	27.6086	0.0043
P	210	97	−89	316.5511	146.2116	−134.1549	209.8359	96.9210	−88.9288	125.7533	0.1955
Q	−77	−89	190	−77.0022	−89.0042	190.0120	−142.6190	−164.8485	351.9293	0.0129	190.4730
R	−98	22	168	−97.9957	21.9991	167.9944	−236.6807	53.1325	405.7424	0.0071	276.9892
S	99	−289	190	98.9870	−288.9561	189.9724	70.7877	−206.6388	135.8534	0.0535	102.5239

Table 5 Arrival time recorded by sensors in the third example

Sensor	Arrival time recorded by sensor /s				
	O	P	Q	R	S
A	0.049163	0.092888	0.052240	0.031098	0.101874
B	0.087733	0.105778	0.019478	0.039343	0.052428
D	0.011358	0.065270	0.065807	0.054822	0.091209
F	0.118461	0.089756	0.084068	0.086380	0.097143
H	0.080405	0.033577	0.104970	0.094441	0.122503
G	0.108374	0.060731	0.093107	0.097467	0.085892

Table 6 Comparison between actual and calculated coordinates and errors of absolute distance in the third example

AE event	Actual coordinate/m			Calculated coordinate/m						Error of absolute distance/m	
				Solution 1			Solution 2				
	x	y	z	x_{p1}	y_{p1}	z_{p1}	x_{p2}	y_{p2}	z_{p2}	Solution 1	Solution 2
O	110	200	180	120.4378	218.9831	197.0801	110.0057*	200.0151*	180.0092*	27.5869	0.0186
P	210	97	−89	316.3407	146.1182	−134.0690	209.9725*	96.9866*	−88.9889*	125.5076	0.0325
Q	−77	−89	190	−76.9941*	−88.9993*	189.9942*	−142.6295	164.8688	351.9590	0.0083	308.2001
R	−98	22	168	−97.9964*	21.9992*	167.9961*	−236.6779	−53.1317	405.7389	0.0054	285.3000
S	99	−289	190	98.9718*	−288.9093*	189.9414*	70.7997	206.6721	135.8751	0.1116	499.4153

*: Reasonable solutions

from Table 6 that one set of the location results of the proposed analytical solutions are fully consistent with the actual coordinates.

3.2 Experimental validation

The AE tests were carried out in a cuboid of granite rock using five AE sensors. The sensor coordinates are *A*(−60, 80, 90), *B*(−60, −80, 90), *C*(60, −80, 90), *D*(60, 80, 90), *E*(−60, 80, −90). AE/MS sources are *O*(60, 30, 40), *P*(28, −80, 38) and *Q* (−29, 80, 58) (all coordinates have the length unit of cm). The arrival time recorded by sensors is listed in Table 7, and the accuracy of time is 10^{-6} s. By using the proposed analytical solution to calculate the AE/MS source coordinates, coordinate values of the five sensor and arrival time of the five sensors for five events are taken into equations of ASI, ASII and ASIII. The coordinate values of acoustic emission events can be resolved. The actual and calculated results are listed in Table 8. It can be seen from Table 8 that one set of the location results of the proposed analytical solutions are fully consistent with the actual coordinates.

It can be seen from the above validated examples that there are two groups of solutions using the proposed analytical solutions. One is the real and correct solution, the other one is meaningless solution. The problem is how to select the real solution and cancel the meaningless solution. The checking calculation with arrival time of the sixth sensor is an efficient approach to select a reasonable solution. For example, the arrival time of six sensors (i.e. sensor *G*) is listed in Table 5. The solutions in Table 6 are obtained only using the arrival time of the first five sensors. We can use arrival time t_{p6} and coordinates of the sixth sensor *G* to select the reasonable solution. The distance *D* between the solved source and sensor *G* can be calculated according to the distance formula between two points in space. v_p can be solved using Eq. (39). According to t_{p10}, the original time $t_{original}$ of the event can be obtained by taking the subtraction of t_{p1} and t_{p10}, then the reasonable solution should meet the following criterion:

$$D = v_p(t_{p6} - t_{original}) \tag{58}$$

Taking the values of sensor *G* into Eq. (58), we can easily get the reasonable solutions which are listed in Table 6.

Table 7 Arrival time recorded by sensors for three groups of AE tests

Sensor	Arrival time for ASI/s			Sensor	Arrival time for ASII/s			Sensor	Arrival time for ASIII/s		
	O	*P*	*Q*		*O*	*P*	*Q*		*O*	*P*	*Q*
A	0.060279	0.090380	0.160090	*A*	0.080279	0.100381	0.190090	*A*	0.010279	0.110380	0.280089
B	0.060342	0.090205	0.160333	*B*	0.080341	0.100205	0.190333	*B*	0.010341	0.110205	0.280332
C	0.060242	0.090122	0.160372	*D*	0.080142	0.100343	0.190189	*D*	0.010142	0.110343	0.280190
D	0.060142	0.090343	0.160190	*E*	0.080368	0.100447	0.190303	*F*	0.010417	0.110312	0.280441
E	0.060369	0.090447	0.160303	*F*	0.080418	0.100311	0.190441	*H*	0.010279	0.110415	0.280347

Table 8 Results and comparison of AE experiments

Solution	Event	Actual coordinate/cm			Calculated coordinate/cm					
					Solution 1			Solution 2		
		x	*y*	*z*	*x*	*y*	*z*	*x*	*y*	*z*
ASI	*O*	60	30	40	185.39	92.97	123.03	57.71*	28.94*	38.29*
	P	28	−80	38	57.41	−164.31	79.39	28.39*	−81.27*	39.27*
	Q	−29	80	58	−29.32*	81.54*	58.94*	−48.31	134.39	97.14
ASII	*O*	60	30	40	205.63	97.98	129.91	54.13*	−25.79*	34.19*
	P	28	−80	38	58.60	−164.69	77.62	28.99*	81.48*	38.40*
	Q	−29	80	58	−28.69*	80.18*	58.03*	−48.89	−136.66	98.90
ASIII	*O*	60	30	40	178.14	89.12	118.76	59.95*	29.99*	39.97*
	P	28	−80	38	54.51	−155.35	74.25	30.25*	−86.20*	41.20*
	Q	−29	80	58	−29.19*	79.58*	58.33*	−49.90	136.06	99.72

*: Reasonable solutions

4 Conclusions

1) The sensor location coordinates were simplified as a cuboid monitoring network. Different locations of sensors on upper and lower surfaces were considered and used to establish nonlinear equations.

2) Based on the proposed functions of time difference of arrivals, the analytical solutions were obtained using five sensors under two networks. The proposed analytical solutions were validated using authentic data. The results show that the proposed analytical solution is reasonable and a set of the resolved solutions are consistent with the authentic results.

3) The sixth sensor is needed to determine the unique solution of the source location. Based on a cuboid monitoring network of sensor location, the method can locate the coordinates of AE/MS source only using simple four arithmetic operations. The method highlights three outstanding advantages of without using iterative solution, without initial evaluated hypocenter coordinates and without pre-measured velocity or pre-given velocity boundary conditions.

References

[1] ABDUL-WAHED M K, AL HEIB M, SENFAUTE G. Mining-induced seismicity: Seismic measurement using multiplet approach and numerical modeling [J]. Int J Coal Geol, 2006, 66(1−2): 137−147.

[2] DONG L J, LI X B, XIE G N. Nonlinear methodologies for identifying seismic event and nuclear explosion using random forest, support vector machine, and naive bayes classification [J]. Abstract and Applied Analysis, 2014, 2014: 459137.

[3] DONG L J, LI X B. A microseismic/acoustic emission source location method using arrival times of PS waves for unknown velocity system [J]. International Journal of Distributed Sensor Networks, 2013, 2013: 307489.

[4] LI X B, DONG L J. Comparison of two methods in acoustic emission source location using four sensors without measuring sonic speed [J]. Sensor Lett, 2011, 9(5): 2025−2029.

[5] DONG Long-jun, LI Xi-bing, TANG Li-zhong, Gong Feng-qiang. Mathematical functions and parameters for microseismic source location without pre-measuring speed [J]. Chinese Journal of Rock Mechanics and Engineering, 2011, 30(10): 2057−2067.(in Chinese)

[6] GE M. Source location error analysis and optimization methods [J]. Journal of Rock Mechanics and Geotechnical Engineering, 2012, 4(1): 1−10.

[7] DONG Long-jun, LI Xi-bing, PENG Kang. Prediction of rockburst classification using random Forest [J]. Transactions of Nonferrous Metals Society of China, 2013, 23(2): 472−477.

[8] CHEN B R, FENG X T, ZENG X, XIAO Y Y, ZHANG Z M, MING H J, WEI G L. Real-time microseismic monitoring and its characteristic analysis during TBM tunneling in deep-buried tunnel [J]. Chinese Journal of Rock Mechanics and Engineering, 2011, 30(2): 275−283. (in Chinese)

[9] CHENG Wu-wei, WANG Wen-you, HUANG Shi-qiang, MA Peng. Acoustic emission monitoring of TBM-excavated headrace tunnels of Jinping II hydropower station [J]. Journal of Rock Mechanics and Geotechnical Engineering, 2013, 5(6): 486−494.

[10] TANG Chun-an, WANG Ji-min, ZHANG Jing-jian. Preliminary engineering application of microseismic monitoring technique to rockburst prediction in tunneling of Jinping II project [J]. Journal of Rock Mechanics and Geotechnical Engineering, 2010, 2(3): 193−208.

[11] DONG L J, LI X B. Comprehensive models for evaluating rockmass stability based on statistical comparisons of multiple classifiers [J]. Mathematical Problems in Engineering, 2013, 2013: 395096.

[12] WANG Ji-min, ZENG Xiong-hui, ZHOU Ji-fang. Practices on rockburst prevention and control in headrace tunnels of Jinping II hydropower station [J]. Journal of Rock Mechanics and Geotechnical Engineering, 2012, 4(3): 258−268.

[13] DONG L J, LI X B, MA C D, ZHU W. Comparisons of Logistic regression and Fisher discriminant classifier to seismic event identification [J]. Disaster Advances, 2013, 6: s1−s8.

[14] LI X B, DONG L J, ZHAO G Y, HUANG M, LIU A H, ZENG L F, DONG L, CHEN G H. Stability analysis and comprehensive treatment methods of landslides under complex mining environment—A case study of Dahu landslide from Linbao Henan in China [J]. Safety Sci, 2012, 50(4): 695−704.

[15] DONG Long-jun, LI Xi-bing, ZHAO Guo-yan, GONG Feng-qiang. Fisher discriminant analysis model and its application to predicting destructive effect of masonry structure under blasting vibration of open-pit mine [J]. Chinese Journal of Rock Mechanics and Engineering, 2009, 28(4): 750−756. (in Chinese)

[16] DONG L J, LI X B, XU M, LI Q Y. Comparisons of random forest and support vector machine for predicting blasting vibration characteristic parameters [J]. Procedia Engineering, 2011, 26: 1772−1781.

[17] GEIGER L. Probability method for the determination of earthquake epicenters from the arrival time only [J]. Bulletin St Louis University, 1910, 8: 60−71.

[18] LI Qi-yue, DONG Long-jun, LI Xi-bing, YIN Zhi-qiang, LIU Xi-ling. Effects of sonic speed on location accuracy of acoustic emission source in rocks [J]. Transactions of Nonferrous Metals Society of China, 2011, 21(12): 2719−2726.

[19] LI X B, DONG L J. An efficient closed-form solution for acoustic emission source location in three-dimensional structures [J]. AIP Advances, 2014, 4(2): 027110.

[20] KUNDU T. Acoustic source localization [J]. Ultrasonics, 2014, 54 (1): 25–38.

[21] CIAMPA F, MEO M, BARBIERI E. Impact localization in composite structures of arbitrary cross section [J]. Structural Health Monitoring, 2012, 11(6): 643–655.

[22] NAKATANI H, KUNDU T, TAKEDA N. Improving accuracy of acoustic source localization in anisotropic plates [J]. Ultrasonics, 2014, 54(7): 1776−1778.

[23] PAVLIS G L. Appraising earthquake hypocenter location errors: A complete, practical approach for single-event locations [J]. Bulletin of the Seismological Society of America, 1986, 76(6): 1699−1717.

[24] PAVLIS G L, BOOKER J R. The mixed discrete-continuous inverse problem: Application to the simultaneous determination of earthquake hypocenters and velocity structure [J]. Journal of Geophysical Research, 1980, 85(B9): 4801−4810.

[25] WALDHAUSER F, ELLSWORTH W L. A double-difference earthquake location algorithm: Method and application to the northern Hayward fault, California [J]. Bulletin of the Seismological Society of America, 2000, 90(6): 1353−1368.

[26] DONG L J, LI X B, XIE G N. An analytical solution for acoustic emission source location for known P wave velocity system [J]. Mathematical Problems in Engineering, 2014, 2014: 290686.

[27] DONG Long-jun, LI Xi-bing. Three-dimensional analytical solution of acoustic emission or microseismic source location under cube monitoring network [J]. Transactions of Nonferrous Metals Society of China, 2012, 22(12): 3087−3094.

无需预先测速的长方体监测网络声发射源三维解析定位方法

董陇军[1,2], 李夕兵[1], 周子龙[1], 陈光辉[1], 马 举[1]

1. 中南大学 资源与安全工程学院，长沙 410083；

2. Australian Centre for Geomechanics, The University of Western Australia, Perth 6009, Australia

摘 要：为得到未知波速结构声发射源定位坐标求解的解析解，将传感器阵列简化为长方体，以求得最小监测网络下的声发射源定位解析解。考虑传感器在长方体表面不同位置的各种情形，建立对应的定位控制非线性方程组。根据建立的方程组和到时差，将监测网络分为 3 种情况，分别求得未知波速情况下采用 5 个传感器进行定位的声发射源定位解析解。将得到的声发射源定位解析解应用到数值和声发射试验中进行验证。结果显示，所求得的解析解避免了预先测定波速与迭代算法求解给定位带来的误差，定位结果与真实坐标一致。

关键词：声发射；震源；传感器；定位；解析解

(Edited by Wei-ping CHEN)